POWER CONTROL SYSTEM MODIFICATION AND SIMULATION OF CPR1000

Xinyu WEI, Li WANG and Fuyu ZHAO
Department of nuclear science and technology
Xi'an Jiaotong University
No.28, Xianning West Road, Xi'an, Shaanxi, 710049, P.R. China
xyuwei@xjtu.edu.cn, liwang@xjtu.edu.cn, fyzhao@mail.xjtu.edu.cn

ABSTRACT

Due to development of electric power system, the proportion of nuclear power and its needs for load follow operation have become large. Then there would be higher requirements to the power control ability of the nuclear power system. The axial power distribution may change a lot in the operation process and be affected by many factors. In particular, as the power change is performed within a load follow maneuver, several modifications occur in the core from a neutronic view point: the fuel and moderator temperature change, the xenon concentration and distribution are modified, the power distribution skewed axially, etc. These changes need to be adequately counterbalanced to keep both the core critical and the power distribution acceptable. The traditional approach in pressurized water reactors (PWRs) is compensating for the reactivity change due to the power variation by adjusting the soluble boron concentration and moving a limited number of control banks. However, dilution/boronation strategy becomes expensive for short time changes and leads to large volume of liquid effluent, so it is eager about a capability to perform load follow operation without changing soluble boron concentration. CPR1000, one of the main reactor types in China national development, is taken an example in this paper. It adopts a control method called Mode G, using G banks, N banks, R bank and soluble boron to perform the load follow control. According to the analysis of the physics and thermal principle, a two-node dynamic function model was built, putting the coupling coefficient and mutual influence into consideration. By the calculation of these transient parameter values which are acquired by the steady-state calculation of single channel, the core system model of CPR1000 is established. In order to carry out the load follow operation without the boron adjustment, named as BTP mode, the control banks were regrouped to control the average temperature by M banks and axial offset by AO bank. After that, the average temperature control system (M banks control system) and the axial offset control system (AO bank control system) are built. When the optimal control system is connected to the core model simulation platform, the BTP mode load follow operation of the modified CPR1000 is simulated in the end of the paper.

Key words: Load Follow, Boron Adjustment, CPR1000

1 INTRODUCTION

The development of nuclear power brings more attention to advanced reactor designs, performance and flexibility, including their enhanced load follow capability. The most concerned in nuclear power system is power and power distribution. The radial power distribution, which wouldn't change a lot in the operation process, usually can be adjusted by symmetrically lay outing the fuel rods, flammable poison rods and control rods, and the reasonable program design of rods movement. The axial power distribution may change a lot in the operation process and be affected by many factors. In particular, as the power change is performed within a load follow maneuver, several modifications occur in the core from a neutronic view point: the fuel and moderator temperature change, the xenon concentration and distribution are modified, the power distribution skewed axially, etc.[1]. These changes need to be adequately counterbalanced to keep both the core critical and the power distribution acceptable. The traditional approach in pressurized water reactors (PWRs) is compensating for the reactivity change due to the power variation by adjusting the soluble boron concentration and moving a limited number of control banks[2]. However, dilution/boronation strategy becomes expensive for short time changes and leads to large volume of liquid effluent, so it is eager about a capability to perform load follow operation without changing soluble boron concentration, called BTP mode[3], desirable for a range of reactor designs.

CPR1000, one of the main reactor types in China national development, was taken an example. According to the analysis of the physics and thermal principle, a two-node dynamic function model was built, putting the coupling coefficient and mutual influence into consideration. By the calculation of these transient parameter values which are acquired by the steady-state calculation of single channel, the core system model of CPR1000 is established in section 2. In order to realize the core model's load follow operation, the control banks are redesigned without changing the core structure. After that, the average temperature control system (M banks control system) and the axial offset control system (AO bank control system) are built in section 3. When the optimal control system is connected to the core model simulation platform, the BTP mode load follow operation of the modified CPR1000 is simulated in section 4.

2 CORE SYSTEM MODELING

Point kinetics model is not suitable for a large reactor, because in that flux shape undergoes appreciable variation with time. The behavior of large reactor core, for example the CPR1000, could be explained with reasonable accuracy by spatial model such as the two-node model dividing the reactor core into two regions, considering the influence of the two-node's neutron coupling (shown in Fig.1).

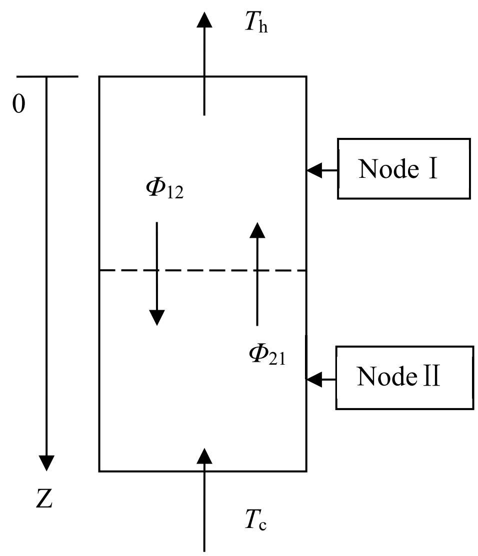

Fig.1 Two-node Dynamic Model.

In Fig.1, the axial direction is chosen as the z coordinate axes, with the top of the core as a origin point. Tc and Th is the inlet and outlet temperature of the core coolant. Φ21 is the neutron current from NodeI to NodeII through the section and Φ12 is the neutron current from NodeII to NodeI.

2.1 Dynamic equations

The core of nuclear reactor is divided into two equal halves (bottom and top). Simplified dynamic equations for each half of core were obtained through neutron diffusion equations [4]. Two halves are coupled together through neutron diffusion. The following set of coupled differential equations represents two-point neutron dynamic model of nuclear reactor.

Node I

$$\frac{dn_1}{dt} = \frac{\rho_1 - \beta}{l_1} n_1 + \sum_{i=1}^{6} \lambda_i D_{i1} - F_{21} n_1 + F_{12} n_2 \tag{1}$$

$$\frac{dD_{i1}}{dt}=\frac{\beta_i}{l_1}n_1-\lambda_i D_{i1},\ i=1,2,\ldots,6 \tag{2}$$

Node II

$$\frac{dn_2}{dt}=\frac{\rho_2-\beta}{l_2}n_2+\sum_{i=1}^{6}\lambda_i D_{i2}-F_{12}n_2+F_{21}n_1 \tag{3}$$

$$\frac{dD_{i2}}{dt}=\frac{\beta_i}{l_2}n_2-\lambda_i D_{i2},\ i=1,2,\ldots,6 \tag{4}$$

where the subscripts 1,2 represent for NodeI and NodeII, respectively, Di1 and Di2 are the each group delayed neutron precursor concentrations in NodeI and NodeII, respectively, F12 means neutron coupling coefficient from NodeII to NodeI and F21 means neutron coupling coefficient from NodeI to NodeII.

$$F_{12}=F_{21}=\frac{4Dv}{l^2} \tag{5}$$

As shown in Fig.2, an average coolant channel is chosen as a research object to derivate the thermal dynamic functions. p is the distance of the coolant channel, ru is the fuel radius, rci and rcs are the inside and surface radius of the cladding, respectively.

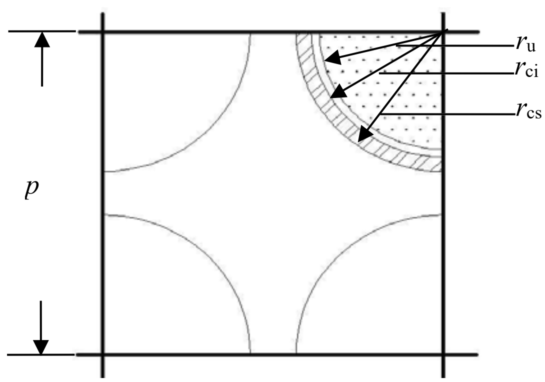

Fig.2 An Average Coolant Channel.

The fuel and the coolant temperature are described by the following equations[4].
Node I

$$\frac{dT_{f1}}{dt}=A_1 n_1-\frac{1}{\tau_{f1}}(T_{f1}-T_{m1}) \tag{6}$$

$$\frac{dT_{m1}}{dt}=\frac{1}{\tau_{m1}}(T_{f1}-T_{m1})-\frac{1}{\tau_{01}}(T_k-T_c) \tag{7}$$

Node II

$$\frac{dT_{f2}}{dt}=A_2 n_2-\frac{1}{\tau_{f2}}(T_{f2}-T_{m2}) \tag{8}$$

$$\frac{dT_{m2}}{dt}=\frac{1}{\tau_{m2}}(T_{f2}-T_{m2})-\frac{1}{\tau_{02}}(T_h-T_k) \tag{9}$$

where, the subscript *f* represents for the variables about fuel and *m* for moderator, T_h, T_k, T_c are the outlet, middle part, inlet temperatures of the core, respectively, actually T_k indicates both the outlet temperature of NodeⅠ and the inlet temperature of NodeⅡ. $A, \tau_f, \tau_m, \tau_0$ are identified as:

$$
\begin{aligned}
A_1 &= \frac{\xi_1}{c_{f1}d_{f1}} & A_2 &= \frac{\xi_2}{c_{f2}d_{f2}} \\
\tau_{f1} &= \frac{c_{f1}d_{f1}r_u^2}{2k_{f1}r_{f1}} & \tau_{f2} &= \frac{c_{f2}d_{f2}r_u^2}{2k_{f2}r_{f2}} \\
\tau_{m1} &= \frac{c_{m1}d_{m1}A_{m1}}{2\pi k_{f1}r_{f1}} & \tau_{m2} &= \frac{c_{m2}d_{m2}A_{m2}}{2\pi k_{f2}r_{f2}} \\
\tau_{01} &= \frac{l_1 d_{m1} Am_1}{W_{m1}} & \tau_{02} &= \frac{l_2 d_{m2} Am_2}{W_{m2}}
\end{aligned}
\tag{10}
$$

They are depended on the thermal capacity and conductivity of the fuel and coolant, whose values are obtained from the CPR1000 reactor parameters.

The Xenon concentrations at each node are governed by a set of I-Xe coupled differential dynamic equations [5]. Similarly, the iodine and xenon concentrations varying are represented as:

Node I

$$\frac{dn_{I1}}{dt} = \gamma_I \Sigma_{f1} v_1 n_1 - \lambda_I n_{I1} \tag{11}$$

$$
\begin{aligned}
\frac{dn_{Xe1}}{dt} = {} & \gamma_{Xe}\Sigma_{f1} v_1 n_1 + \lambda_I n_{I1} \\
& - (\lambda_{Xe} + \sigma_a^{Xe} v_1 n_1) n_{Xe1}
\end{aligned}
\tag{12}
$$

Node II

$$\frac{dn_{I2}}{dt} = \gamma_I \Sigma_{f2} v_2 n_2 - \lambda_I n_{I2} \tag{13}$$

$$
\begin{aligned}
\frac{dn_{Xe2}}{dt} = {} & \gamma_{Xe}\Sigma_{f2} v_2 n_2 + \lambda_I n_{I2} \\
& - (\lambda_{Xe} + \sigma_a^{Xe} v_2 n_2) n_{Xe2}
\end{aligned}
\tag{14}
$$

where n_I, n_{Xe} are the average concentrations of ^{135}I and ^{135}Xe, respectively, γ_I, γ_{Xe} the respective fission yields, λ_I, λ_{Xe} the respective decay constants, σ_a^{Xe} the xenon microscopic absorption cross section and Σ_f the macroscopic fission cross section.

Reactivity changing is derived from control rods insertion, fuel temperature feedback, moderator temperature feedback, xenon concentration and the amount of soluble boron, etc.[6]. Then the two-node core equations relating reactivity are:

Node I

$$
\begin{aligned}
\rho_1 = {} & \rho_{rod1} + \alpha_{f1}\delta T_{f1} + \alpha_{m1}\delta T_{m1} \\
& + \alpha_{Xe1}\delta n_{Xe1} + \alpha_{B1}\delta n_{B1}
\end{aligned}
\tag{15}
$$

Node II

$$
\begin{aligned}
\rho_2 = {} & \rho_{rod2} + \alpha_{f2}\delta T_{f2} + \alpha_{m2}\delta T_{m2} \\
& + \alpha_{Xe2}\delta n_{Xe2} + \alpha_{B2}\delta n_{B2}
\end{aligned}
\tag{16}
$$

where the symbol δ indicates the deviation of a value from an desired value. n_{B1}, n_{B2} are the average boron concentrations of NodeI and NodeII, respectively. The deviation values in the equations above are defined as followed.

$$
\begin{aligned}
\delta T_{f1} &= T_{f1} - T_{f01} & \delta T_{f2} &= T_{f2} - T_{f02} \\
\delta T_{m1} &= T_{m1} - T_{m01} & \delta T_{m2} &= T_{m2} - T_{m02} \\
\delta n_{Xe1} &= n_{Xe1} - n_{Xe01} & \delta n_{Xe2} &= n_{Xe2} - n_{Xe02} \\
\delta n_{B1} &= n_{B1} - n_{B01} & \delta n_{B2} &= n_{B2} - n_{B02}
\end{aligned}
\tag{17}
$$

where the symbol 0 indicates the steady state value, and T_{f01}, T_{f02}, T_{m01}, T_{m02}, n_{Xe01}, n_{Xe02}, n_{B01}, n_{B02} correspond to the desired values of T_{f1}, T_{f2}, T_{m1}, T_{m2}, n_{Xe1}, n_{Xe2}, n_{B1}, n_{B2}, respectively.

But in our control system design, the function of the soluble boron concentration adjustment is free in a short control circle about a week, so the last term of the equations can be ignored in the reactivity effects.

Node I

$$\rho_1 = \rho_{rod1} + \alpha_{f1}\delta T_{f1} + \alpha_{m1}\delta T_{m1} + \alpha_{Xe1}\delta T_{Xe1} \tag{18}$$

Node II

$$\rho_2 = \rho_{rod2} + \alpha_{f2}\delta T_{f2} + \alpha_{m2}\delta T_{m2} + \alpha_{Xe2}\delta T_{Xe2} \tag{19}$$

2.2 Linearization and Laplace transform

In order to make the equations easier to express and derive, some variables need to get their relative values, these are the ratios of the actual values to the steady- state ones.

$$\begin{aligned} N_1 &= \frac{n_1}{n_{01}} & N_2 &= \frac{n_2}{n_{02}} \\ C_{i1} &= \frac{D_{i1}}{D_{i01}} & C_{i2} &= \frac{D_{i2}}{D_{i02}} \\ I_1 &= \frac{n_{I1}}{n_{I01}} & I_2 &= \frac{n_{I2}}{n_{I02}} \\ Xe_1 &= \frac{n_{Xe1}}{n_{Xe01}} & Xe_2 &= \frac{n_{Xe2}}{n_{Xe02}} \end{aligned} \tag{20}$$

where also, the symbol 0 indicates the steady state value.

Then, to convert the load follow problem of nuclear reactor to the stabilization problem, the deviation values are defined

$$\begin{aligned} \delta N_1 &= N_1 - 1 & \delta N_2 &= N_2 - 1 \\ \delta C_{i1} &= C_{i1} - 1 & \delta C_{i2} &= C_{i2} - 1 \\ \delta I_1 &= I_1 - 1 & \delta I_2 &= I_2 - 1 \\ \delta Xe_2 &= Xe_2 - 1 & \delta Xe_2 &= Xe_2 - 1 \\ \delta\rho_1 &= \rho_1 - \rho_{01} & \delta\rho_2 &= \rho_2 - \rho_{02} \\ \delta T_h &= T_h - T_{h0} & \delta T_k &= T_k - T_{k0} \\ \delta T_c &= T_c - T_{c0} & & \\ \delta\rho_{rod1} &= \rho_{rod1} - \rho_{rod01} & & \\ \delta\rho_{rod2} &= \rho_{rod2} - \rho_{rod02} & & \end{aligned} \tag{21}$$

where also, the symbol δ indicates the deviation of a value from a desired value.

A set of linear equations would be obtained after the normalization for describing the behavior of the reactor in the vicinity of the steady-state operating point as follows:

Node I

$$\begin{aligned} \frac{d\delta N_1}{dt} &= \frac{\rho_{01} - \beta}{l_1}\delta N_1 + \frac{\delta\rho_1}{l_1} + \sum_{i=1}^{6}\frac{\beta_i}{l_1}\delta C_{i1} \\ &\quad - F_{21}\delta N_1 + \frac{n_{02}}{n_{01}}F_{12}\delta N_2 \end{aligned} \tag{22}$$

$$\frac{d\delta C_{i1}}{dt} = \lambda_i\delta N_1 - \lambda_i\delta C_{i1},\ i=1,2,\ldots,6 \tag{23}$$

$$\frac{d\delta T_{f1}}{dt}=A_1 n_{01}\delta N_1-\frac{1}{\tau_{f1}}(\delta T_{f1}-\delta T_{m1}) \tag{24}$$

$$\frac{d\delta T_{m1}}{dt}=\frac{1}{\tau_{m1}}(\delta T_{f1}-\delta T_{m1})-\frac{1}{\tau_{01}}(\delta T_k-\delta T_c) \tag{25}$$

$$\frac{d\delta I_1}{dt}=\gamma_I \Sigma_{f1} v_1 \frac{n_{01}}{n_{I01}}\delta N_1-\lambda_I \delta I_1 \tag{26}$$

$$\begin{aligned}\frac{d\delta Xe_1}{dt}&=\gamma_{Xe}\Sigma_{f1}v_1\frac{n_{01}}{n_{Xe01}}\delta N_1+\lambda_I\frac{n_{I01}}{n_{Xe01}}\delta I_1\\&-\lambda_{Xe}\delta Xe_1-\sigma_a^{Xe}v_1 n_{01}(\delta Xe_1+\delta N_1)\end{aligned} \tag{27}$$

$$\begin{aligned}\delta\rho_1 &= \delta\rho_{rod1}+\alpha_{f1}\delta T_{f1}+\alpha_{m1}\delta T_{m1}\\&+\alpha_{Xe1}n_{Xe01}\delta Xe_1\end{aligned} \tag{28}$$

Node II

$$\begin{aligned}\frac{d\delta N_2}{dt}&=\frac{\rho_{02}-\beta}{l_2}\delta N_2+\frac{\delta\rho_2}{l_2}+\sum_{i=1}^{6}\frac{\beta_i}{l_2}\delta C_{i2}\\&-F_{12}\delta N_2+\frac{n_{01}}{n_{02}}F_{21}\delta N_1\end{aligned} \tag{29}$$

$$\frac{d\delta C_{i2}}{dt}=\lambda_i\delta N_2-\lambda_i\delta C_{i2},\ i=1,2,\ldots,6 \tag{30}$$

$$\frac{d\delta T_{f2}}{dt}=A_2 n_{02}\delta N_2-\frac{1}{\tau_{f2}}(\delta T_{f2}-\delta T_{m2}) \tag{31}$$

$$\frac{d\delta T_{m2}}{dt}=\frac{1}{\tau_{m2}}(\delta T_{f2}-\delta T_{m2})-\frac{1}{\tau_{02}}(\delta T_h-\delta T_k) \tag{32}$$

$$\frac{d\delta I_2}{dt}=\gamma_I\Sigma_{f2}v_2\frac{n_{02}}{n_{I02}}\delta N_2-\lambda_I\delta I_2 \tag{33}$$

$$\begin{aligned}\frac{d\delta Xe_2}{dt}&=\gamma_{Xe}\Sigma_{f2}v_2\frac{n_{02}}{n_{Xe02}}\delta N_2+\lambda_I\frac{n_{I02}}{n_{Xe02}}\delta I_2\\&-\lambda_{Xe}\delta Xe_2-\sigma_a^{Xe}v_2 n_{02}(\delta Xe_2+\delta N_2)\end{aligned} \tag{34}$$

$$\begin{aligned}\delta\rho_2 &= \delta\rho_{rod2}+\alpha_{f2}\delta T_{f2}\\&+\alpha_{m2}\delta T_{m2}+\alpha_{Xe2}n_{Xe02}\delta Xe_2\end{aligned} \tag{35}$$

In order to obtain the core dynamic simulation model, Laplace transform of Eq.(22) to (35) are needed.

NodeI

$$\begin{aligned}(s+F_{21}+\frac{\beta-\rho_{01}}{l_1})\delta N_1(s)&=\frac{1}{l_1}\delta\rho_1(s)\\+\frac{n_{02}}{n_{01}}F_{12}\delta N_2(s)&+\sum_{i=1}^{6}\frac{\beta_i}{l_1}\delta C_{i1}(s)\end{aligned} \tag{36}$$

$$(s+\lambda_i)\delta C_{i1}(s)=\lambda_i\delta N_1(s) \tag{37}$$

$$(s+\frac{1}{\tau_{f1}})\delta T_{f1}(s)=A_1 n_{01}\delta N_1(s)+\frac{1}{\tau_{f1}}\delta T_{m1}(s) \quad (38)$$

$$(s+\frac{1}{\tau_{m1}}+\frac{2}{\tau_{01}})\delta T_{m1}(s)=\frac{1}{\tau_{m1}}\delta T_{f1}(s)+\frac{2}{\tau_{01}}\delta T_c(s) \quad (39)$$

$$\delta T_{m1}(s)=\frac{\delta T_c(s)+\delta T_k(s)}{2} \quad (40)$$

$$(s+\lambda_I)\delta I_1(s)=\gamma_I\Sigma_{f1}v_1\frac{n_{01}}{n_{I01}}\delta N_1(s) \quad (41)$$

$$(s+\lambda_{Xe}+\sigma_a^{Xe}v_1 n_{01})\delta Xe_1(s)=\lambda_I\frac{n_{I01}}{n_{Xe01}}\delta I_1(s)+(\gamma_{Xe}\Sigma_{f1}v_1\frac{n_{01}}{n_{Xe01}}-\sigma_a^{Xe}v_1 n_{01})\delta N_1(s) \quad (42)$$

$$\delta\rho_1(s)=\delta\rho_{rod1}(s)+\alpha_{f1}\delta T_{f1}(s)+\alpha_{m1}\delta T_{m1}(s)+\alpha_{Xe1}n_{Xe01}\delta Xe_1(s) \quad (43)$$

Node II

$$(s+F_{12}+\frac{\beta-\rho_{02}}{l_2})\delta N_2(s)=\frac{1}{l_2}\delta\rho_2(s)+\frac{n_{01}}{n_{02}}F_{21}\delta N_1(s)+-\sum_{i=1}^{6}\frac{\beta_i}{l_2}\delta C_{i2}(s) \quad (44)$$

$$(s+\lambda_i)\delta C_{i2}(s)=\lambda_i\delta N_2(s) \quad (45)$$

$$(s+\frac{1}{\tau_{f2}})\delta T_{f2}(s)=A_2 n_{02}\delta N_2(s)+\frac{1}{\tau_{f2}}\delta T_{m2}(s) \quad (46)$$

$$(s+\frac{1}{\tau_{m2}}+\frac{2}{\tau_{02}})\delta T_{m2}(s)=\frac{1}{\tau_{m2}}\delta T_{f1}(s)+\frac{2}{\tau_{02}}\delta T_k(s) \quad (47)$$

$$\delta T_{m2}(s)=\frac{\delta T_k(s)+\delta T_h(s)}{2} \quad (48)$$

$$(s+\lambda_I)\delta I_2(s)=\gamma_I\Sigma_{f1}v_1\frac{n_{01}}{n_{I01}}\delta N_2(s) \quad (49)$$

$$(s+\lambda_{Xe}+\sigma_a^{Xe}v_2n_{02})\delta Xe_2(s)=\lambda_I\frac{n_{I02}}{n_{Xe02}}\delta I_2(s)$$
$$+(\gamma_{Xe}\Sigma_{f2}v_2\frac{n_{02}}{n_{Xe02}}-\sigma_a^{Xe}v_2n_{02})\delta N_2(s) \tag{50}$$

$$\delta\rho_2(s) = \delta\rho_{rod2}(s) + \alpha_{f2}\delta T_{f2}(s)$$
$$+ \alpha_{m2}\delta T_{m2}(s)+ \alpha_{Xe2}n_{Xe02}\delta Xe_2(s) \tag{51}$$

Axial offset (*AO*) [7] is defined to express the core power peaking

$$AO=\frac{P_2-P_1}{P_1+P_2}=\frac{P_2-P_1}{P} \tag{52}$$

AO, easily measured on-line via ex-core instrumentation, reduces the complexity of the problem and provides an efficient practical mean to control the reactor power distribution.

2.3 Core model simulation

The following dates shown in Table 1 are the steady state calculation parameters and results of load follow operation CPR 1000 core example.

Table 1 Steady state parameters of CPR1000

Parameters	Date	Unit
Core power (*P*)	2875	MW
Input temperature (T_c)	293	℃
Flow quantity (W)	68520	kg/h
Iodine decay constant (λ_I)	2.913e-5	s^{-1}
Xenon decay constant (λ_X)	2.118e-5	s^{-1}
Iodine fission yield (γ_I)	0.063264	%
Xenon fission yield (γ_X)	0.002477	%
neutron flux (φ_0)	[3.4249e14, 4.3004e14]	$m^{-2}s^{-1}$
The steady state reactivity (ρ_0)	[32.69,40.41]	ppm
neutron coupling coefficient ($[F_{12},F_{21}]$)	[68.2455, 55.1972]	
Fuel temperature constant (τ_f)	[2.9243,2.5688]	
Coolant temperature constant (τ_m)	[7.0216,6.5000]	
Temperature constant (τ_0)	[0.4594,0.3990]	
Fuel feedback coefficient (α_f)	[-2.561e-005, -2.453e-005]	
Coolant feedback coefficient (α_m)	[-1.836e-004, -3.587e-004]	
Xenon feedback coefficient (α_X)	[-0.0223, -0.0231]	
the xenon microscopic absorption cross section (σ_α^{Xe})	[2.4596e5, 2.3638 e5]	b

Based on the steady state parameters, the relationship of the variables in the two-node core system is connected and modeled the core dynamic system by MATLAB/SIMULINK. In this simulation system, the input variables are the reactivity of two nodes respectively and the inlet temperature of core, while the output variables are the relative power, outlet temperature of the core, fuel temperature, iodine and xenon concentrations of two nodes, respectively, etc.

3 CONTROL SYSTEM MODELING

3.1Banks redistribution

BTP mode is a new core control method performing load follow operation with boron concentration adjustment free. This mode uses independent mechanical manual control banks (M banks) and axial power control banks (AO bank) to adjust the power and the axial power distribution of the core respectively. During most time of the nuclear fuel circle, load adjustment would be done by this strategy without soluble boron compensating for the negative reactivity. Aim to achieve load follow operation, CPR1000 employs the BTP mode control theory without changing its original structure.

CPR1000 reactor core is comprised of 61 assemblies of control banks, consisting of M banks, AO bank and SD (shut-down) banks. In order to perform the BTP load follow operation, the banks are needed to be regrouped, may as well not change the total number. Fig.3 shows the typical control banks configuration in the redesigned CPR1000 reactor core. The 61 control banks are placed in a checkerboard pattern. 12 gray banks, former G1,G2, are regrouped into three groups, employed in the M1 though M3 banks. 12 Black banks, former N1,N2, are employed in the M4 and M5 bank. The above five banks are designated as M banks. The objective of M banks configuration is to control reactivity/temperature. AO bank is composed of 9 black banks, whose configuration is different due to an increased complement of former R bank (from 8 to 9). At the same time, SD banks' number changes from 25 to 24.

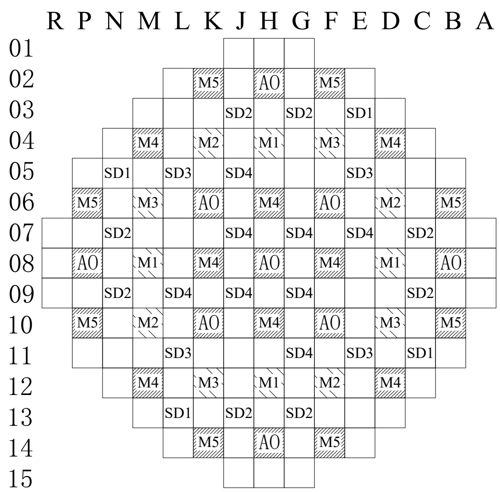

Fig.3 Banks Location in BTP Model.

The control banks have to comply with certain requirements to enable BTP operation while respecting the safety constraints on the plant shut-down. The position and material of the banks are the results of optimizing their negative reactivity worth while minimizing the impact on the power profile during the load follow. The function of the control banks are described in Table 2.

Table 2 Function of the Regrouped Banks

Bank ID		Number	Type	Rodlets material	Worth	Function
Previous	Redesign					
G1	M1	4	Gray	24SS/20SS+4Ag-In-Cd	267	Temperature and power control
G2	M2	4	Gray	24SS	287	
	M3	4	Gray	20SS+4Ag-In-Cd	372	
N1	M4	8	Black	24Ag-In-Cd	579	
N2	M5	8	Black	24Ag-In-Cd	987	
R	AO	9	Black	24Ag-In-Cd	2126	Axial offset control
SA	SD1	4	Black	24Ag-In-Cd		Shutdown
SB	SD2	8	Black	24Ag-In-Cd		
SC	SD3	4	Black	24Ag-In-Cd		
SD	SD4	8	Black	24Ag-In-Cd		
Total		61				

3.2Average temperature control (M banks control)

M banks provide the reactivity control when the power changes. As the control strategy designed, during operation, M1 bank stays in the fully inserted position for an extended period. M1 positioning serves to allow the AO bank insertion, which is needed to shift the *AO* from its reference value at base load condition to the lower value needed for daily operation (the negative reactivity associated with the AO bank insertion needs to be offset by M1 withdrawal to preserve the reactivity balance at hot full power, HFP).

M4 bank and M5 bank with larger worth are also present. This is employed to compensate the larger reactivity defects ensuing from the more demanding maneuvers, i.e., xenon defect due to extended low power operation, power defect involved in transitions to very low powers.

These M banks are tied by a specified overlap relationship and driven by maintaining the reactor power. The moving sequence for the M banks is shown in Fig.4, as well as the banks overlap and their equivalent total length.

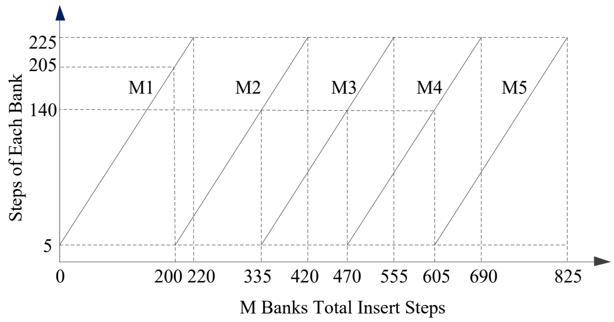

Fig.4 M Banks Overlap Relationship

The average core temperature control is performed by a closed-loop M banks control system, shown in Fig.5.

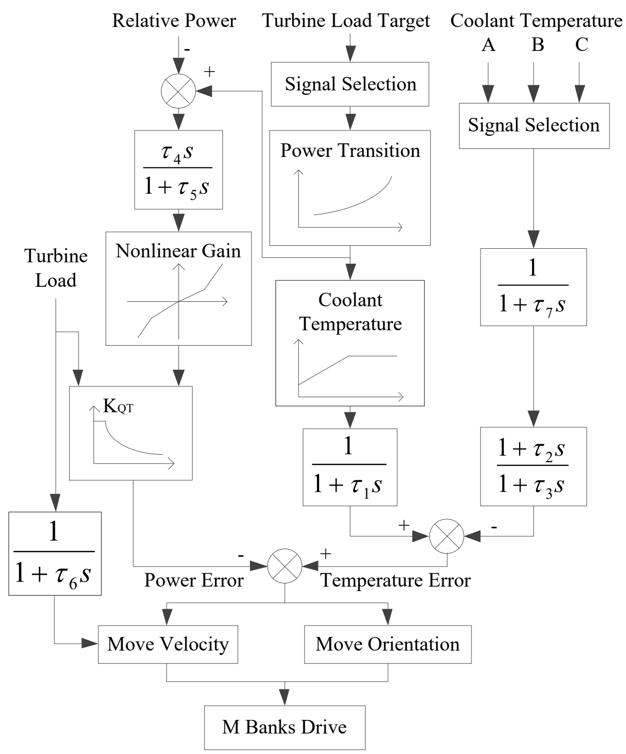

Fig.5 M Banks Control System

The input signals of this system are the core actual power, the maximal value of the turbine's base load and target power, the average temperature value of the core coolant, respectively. During the load follow operation, when the load demand doesn't match the actual power, there would be a temperature error signal changed into the M banks move velocity and orientation (raise or insert) signals by the M banks control unit. Then a logic control device and a power supply generate the driving current pulse to drive the M banks, altering the reactivity in the core, finally regulate the core power.

3.3Axial offset control (AO bank control)

The limitations on the core AO can be analyzed in P-ΔI coordinates, where the axial distribution ΔI is defined as:

$$\Delta I = AO \times P = P_1 - P_2 \qquad (53)$$

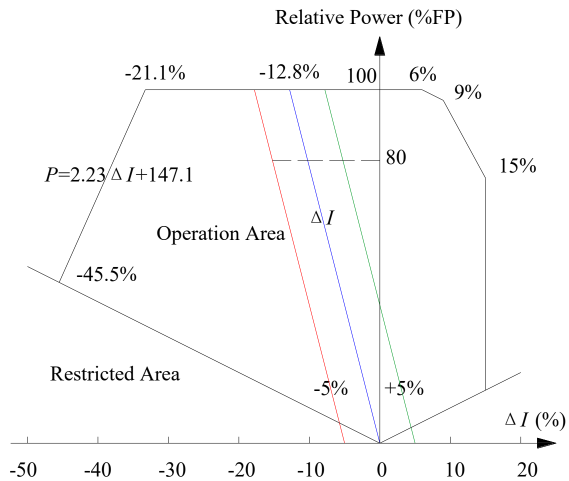

Fig.6 ΔI Band with AO Control

where, P is the relative core thermal power (the ratio of the actual core thermal power to nominal power).
In constant axial offset control (CAOC) strategy[8], the limitations on the core AO value should be shown by two parallel lines in P-ΔI coordinates, controlled by the AO bank regulate strategy. This means that the core working conditions in P-ΔI coordinates would better lie within a certain band (e.g., ±5%) during any power transient, showed in Fig.6.

The AO bank is used to maintain the axial offset at the desired value and ensure safe operation of the reactor during load follow transients, which needs to be withdrawn to counteract the upward movement of the xenon; the capacity of the AO bank to control the axial offset is lost if the point of full extraction is reached. To prevent this issue, when daily maneuvers are anticipated, the AO value is shifted downward from its value at base load condition through deeper insertion of the AO bank. In this way the xenon distribution also shifts downward. The more deeply inserted AO bank and less top skewed xenon distribution concur to preserve the AO control capability of the AO bank upon returning to full power operation. The AO is brought back to its reference base-load value after completion of the maneuver.

The movement of the AO bank is not independent of the M banks movement. In order to avoid the unnecessary reciprocating movement of control rods, it is enforced that only one kind of banks can move at a time, and M banks have the priority. That is to say, during the maneuver circle, M banks are ordered to act first to adjust the core power. Only when the power error comes to the limited tolerance, could the AO bank move to control the axial offset. The axial offset control system is shown in Fig.7.

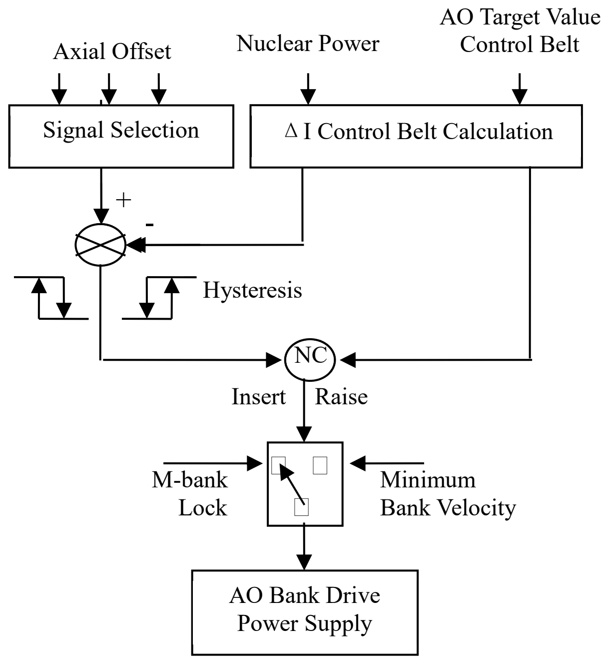

Fig.7 AO Bank Control System

Usually, AO bank stays in the top part of the core. While it is inserted, the power distribution would turn to the bottom half, and to the top half when raised.

4 LOAD FOLLOW SIMULATION

In order to bring about the nuclear power economic operation, achieve the balance of the electric generation and causing, the load follow operation is almost a required feature for PWR. Namely, due to the large inventory of the primary coolant, the dilution/boration strategy becomes not only more expensive, but may additionally be limited by the achievable dilution rate. Therefore, CPR1000 is required to perform load follow without boron concentration adjustment for the basis daily load maneuvers, shown in Fig.8, operated as the followed 24 hours circle: the power is reduced from 100%FP to 80%FP in 3 hours preceded by a 12 hours' full power state and keep the low power for 6 hours, then returns to full power in the left of the day.

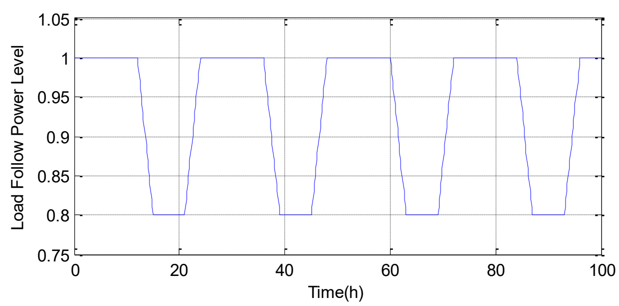

Fig.8 Load Follow Power Change Profile

4.1 Simulation results

The core system (shown in Fig.3) was connected with the bank controller (shown in Fig.6 and 8) by a move velocity – rods reactivity conversion calculation attachment. The load follow simulation reported here refer to the Beginning of Life, Xenon equilibrium (BLX), burnup at 150MWd/tU, M banks with a insertion of 220 steps, and AO bank 35 steps. In this design of control banks insertion surplus at full power, the value of the power axial offset would change to -0.154 from -0.086, as well as the axial distribution ΔI to -15.4%. Four consecutive days of load follow operation are simulated, and the boron adjustment free maneuver is illustrated in Fig.9.

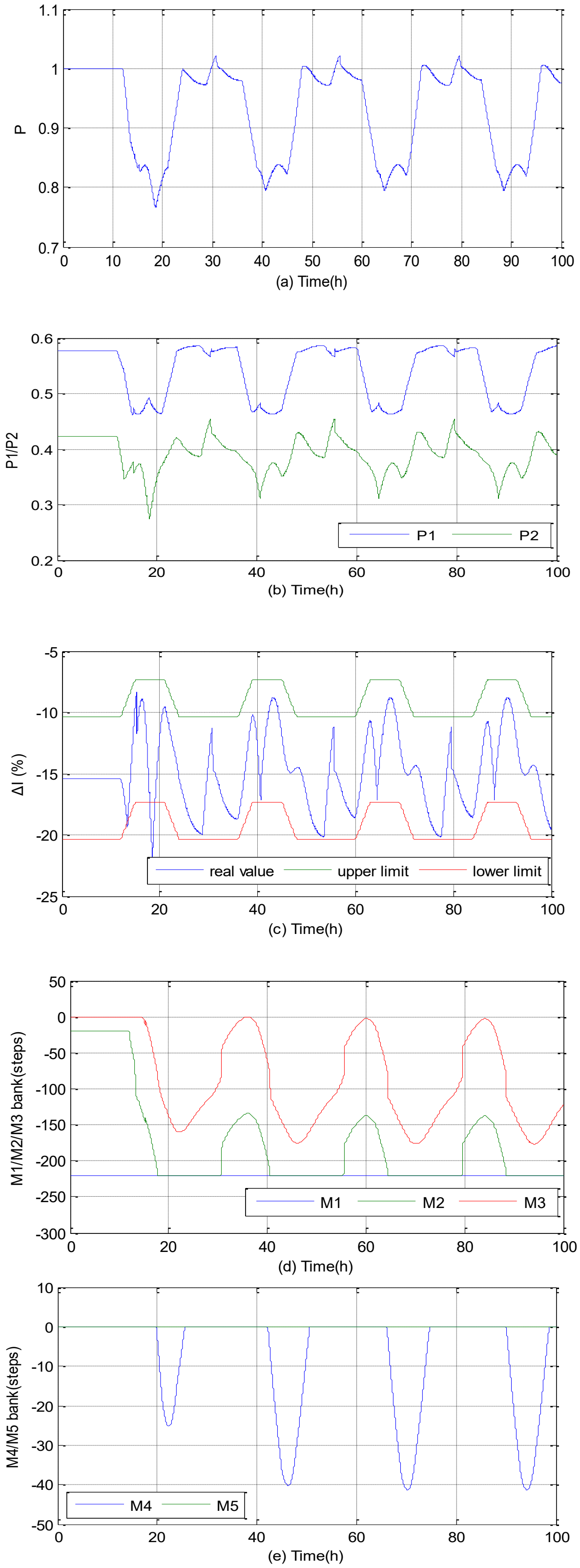
P
(a) Time(h)
P1/P2
P1
P2
(b) Time(h)
ΔI (%)
real value
upper limit
lower limit
(c) Time(h)
M1/M2/M3 bank(steps)
M1
M2
M3
(d) Time(h)
M4/M5 bank(steps)
M4
M5
(e) Time(h)

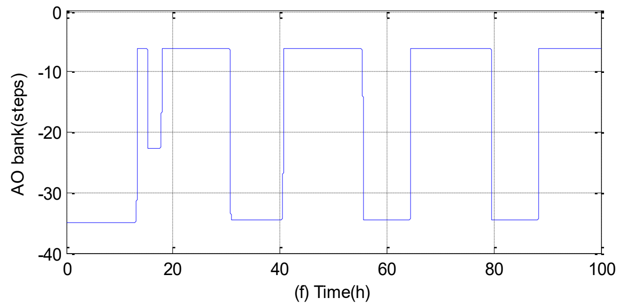

Fig.9

Fig.9 Simulation Results of Load Follow

(a) Real thermal power (b) Two-node real power, respectively. (c) Real core ΔI and ΔI limitations. (d) M1, M2, M3 bank move steps. (e) M4, M5 bank move steps. (f) AO bank move steps.

4.2 APOC calculation

In order to validate the correctness and reasonableness of the core system and the control policy, a one-dimensional in axial computer code, called APOC, is used to calculate nuclear core quasi-steady state parameters with the "12-3-6-3" load maneuvers shown in Fig.8 as the simulation target value. The calculation results are shown in Fig.10 by the same control banks redesign and overlap relationship.

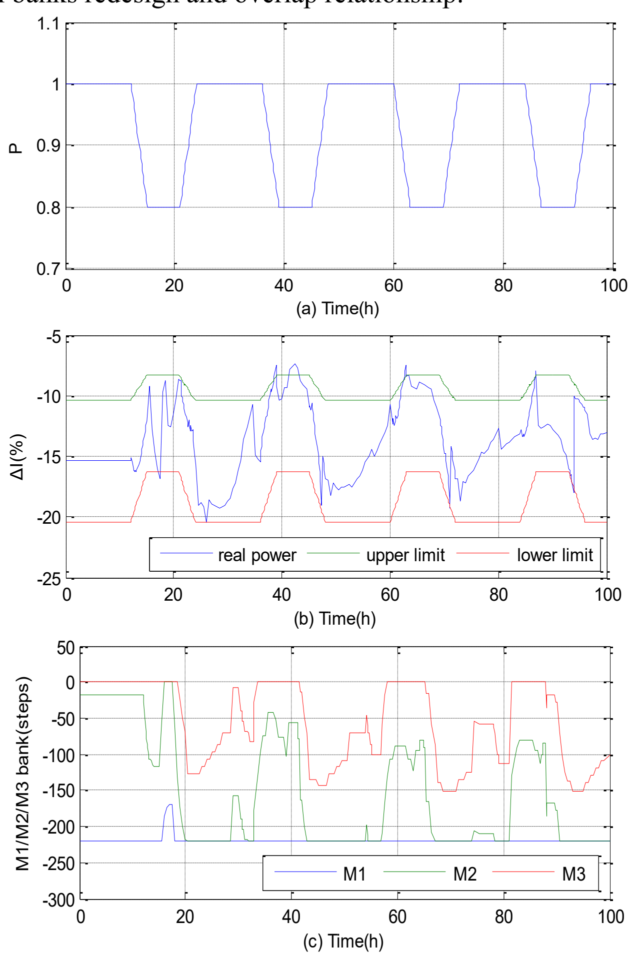

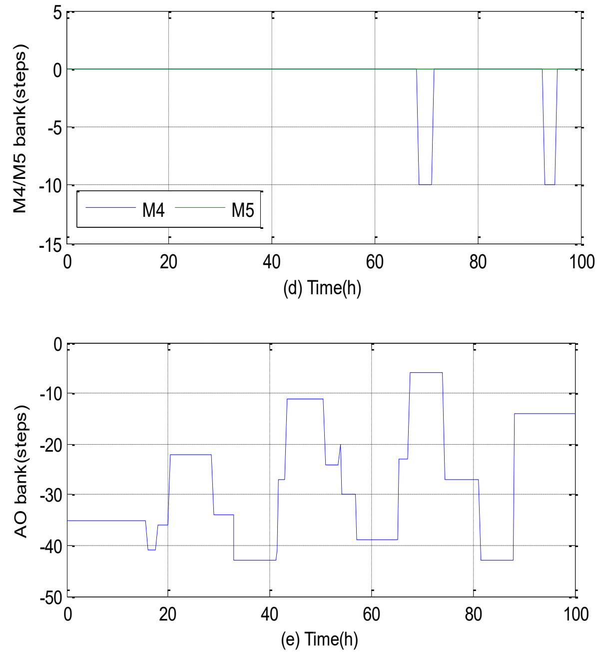

Fig.10 APOC Calculation Results of Load Follow

(a) Real thermal power. (b) Real core ΔI and ΔI limitations. (c) M1, M2, M3 bank move steps. (d) M4, M5 bank move steps. (e) AO bank move steps.

As it shown in Fig.10(a) and (b), the core power and ΔI can be bonded very well, proving the effective of the control system. The control banks movements, getting from the simulation system are compared with the APOC calculation results and shown in Fig.11.

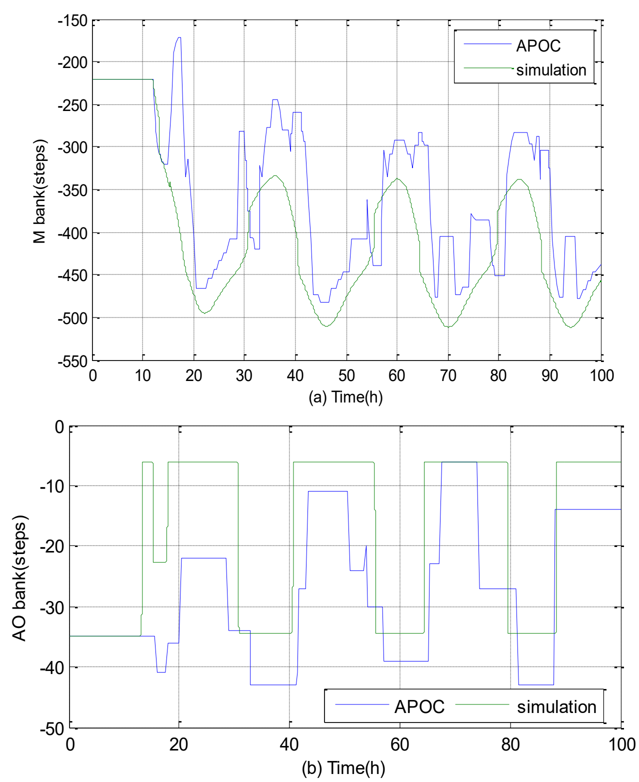

Fig.11 Control Banks Movement Contrast

(a) M banks move comparison. (b) AO bank move comparison.

In the comparison, Fig..11 presents that, at the beginning of the 3-hour reducing ramp in the first circle, there is a temporary raising of the M banks with AO bank inserting in APOC calculation. While in simulation, the control banks drive off in reverse direction. That is because in the simulation control system, the core power is the first variable to be regulated by M banks. That is to say, when the power target goes down, M banks will react first (insert), and AO bank would not operate until ΔI goes out of the lower limit. In other words, the temperature control effect taken by M banks in simulation system is replaced by AO banks in the APOC calculation.

The addition of control system and the differences of calculate logic make some discrepancy in banks movement, but the adjustment trends are similar, especially in the later circles. The results comparison between simulation platform and APOC calculation partly proves that with a redesign of control banks, the CPR1000 has the possibility to realize the load follow operation by BTP operation.

5 CONCLUSION

This paper presents the implementation of operation without boron concentration adjustment to CPR1000. The two-node core dynamic model was presented and the simulation platform was built according to its original physical and thermal parameter. After discussing the basis of boron adjustment free operation, the control banks were regrouped and the operation policy was designed to enable BTP operation. In this work, a robust model predictive control policy to systematically control the power level for load follow had been developed. Simulation results indicate the high performance of this new control design and also showed that axial distribution ΔI and control banks movements were bounded within acceptable limits.

It is finally mentioned that, the CPR1000 has a great possibility to perform the BTP operation control, and follow a daily load cycle after further embellish work by a flexible and convenient core control banks redesign and the boron adjust free operation.

6 ACKNOWLEDGMENTS

This work was supported by the National Science Foundation of China under Grants 11405125; China Postdoctoral Science Foundation Funded Project under Grant 2014M562420, and the Fundamental Research Funds for the Central Universities of China under Grant 2015gjhz09.

7 REFERENCES

[1] Suk-Whun Sohn, Kun-Jai Lee. Development of a boron concentration prediction model using multi-cell simulation of the automatic load follow operation[J]. Annals of Nuclear Energy, 2011, 38

[2] M. Winokur, L. Tepper. Extension of load follow capability of a PWR reactor by optimal control[J]. IEEE Transactions on Nuclear Science, 1984.4, 31(2)

[3] MA Zirong, YAO Zeng-hua. Improvement of M310 PWR——Study on the load follow without boron adjustment[J]. Chinese JournaI of NucIear Science and Engineering, 2004.12, 24(4) (in Chinese)

[4] H.Eliasi, M.B.Menhaj, H.Davilu. Robust nonlinear model predictive control for nuclear power plants in load following operations with bounded xenon oscillations[J]. Nuclear Engineering and Design, 2011, 241

[5] Fausto Franceschini, Bojan Petrovic. Advanced operational strategy for the IRIS reactor: Load follow through mechanical shim[J]. Nuclear Engineering and Design, 2008, 238

[6] Hiroyuki Ukai, Tetsuo Iwazumi. A New Approach to Control of Xenon Spatial Oscillation During Load Follow Operation via Robust Servo Systems [J]. IEEE Transactions on Nuclear Science, 1994, 41(6)

[7] Suoysh, P.J., R.A.Kerr, A.P.Ginsberg, T.Morita, L.R. Scherpereel. Load Follow Demonstrations Employing Constant Axial Offset Power - Distribution Control Procedures. Nuclear Technology, 1976, 31

[8] Mehrdad Boroushaki, Mohammad B. Ghofrani, ect. . Axial offset control of PWR nuclear reactor core using intelligent techniques [J]. Nuclear Engineering and Design, 2004, 227